

Steven K. Chai*, M. A. Wetzel, and D. Koracin
Desert Research Institute, Reno, Nevada

1. INTRODUCTION

The Dynamics and Chemistry of Marine Stratocumulus (DYCOMS-II) field program (Stevens et al. 2003) was designed to improve our understanding of the physics and dynamics of the marine stratocumulus. Nighttime aircraft measurements are used to characterize the entrainment velocities at cloud top, large-scale divergence within the boundary layer, and cloud microphysics.

Uniform cloud fields topping a well-mixed layer were encountered in almost every flight mission. Analyses of the airborne data, with the help of a thermodynamic diagram show that the net radiative loss at cloud top effectively cools the cloud layer resulting in a cooler absolute potential temperature (the temperature of the air, adiabatically lowered to 100 kPa with consideration of the liquid water in the parcel) of the cloud layer than the air below the cloud base. A hydrostatic instability between the cloud layer and the air below is thus created. With some triggering mechanisms, intermittent convection will take place in the marine boundary layer and a uniform absolute potential temperature throughout the boundary layer would then be reestablished. This radiative cooling effect is important not only in cloud dynamics but also in cloud microphysics.

2. DATA ANALYSIS

The cloud-top radiative cooling effect mentioned in the previous section was measured in each research flight. Here we use two vertical soundings observed during the first research flight to demonstrate the scenario. Figure 1 shows the liquid water mixing ratio (r_v) profile observed by NCAR C130 during the first research flight, third profile sounding (RF01/PF03). This is an ascending sounding through the cloud layer. Cloud base and top heights can be easily extracted from this figure. Active cloud-top entrainment can be interpreted from the occasional spikes of smaller r_v values and from the slope of the profile.

Figure 2 shows the profile of the absolute potential temperature (θ_A , solid line) and the wet-bulb potential temperature (θ_W , dashed). The marine boundary layer appears well mixed since both profiles are almost vertical lines. Newly entrained parcels have a slightly higher θ_A and cooler θ_W .

* *Corresponding author address:* Steven K. Chai, Division of Atmospheric Sciences, Desert Research Institute, 2215 Raggio Parkway, Reno, NV 89512-1095; e-mail: chai@dri.edu.

This can be seen more clearly on the θ_W vs. θ_A diagram (Telford and Chai, 1993). In this type of thermodynamic diagram, the θ_W vs. θ_A diagram, the dotted sloping lines are constant total mixing ratio lines and the solid sloping lines are the constant saturation pressure lines. These quantities, as well as θ_A and θ_W , are conserved during adiabatic motion of an air parcel with or without liquid water. Figure 3 shows the RF01/PF03 data on the θ_W vs. θ_A diagram. All the points in the marine boundary layer are clustered in a small region ($\theta_W \approx 13.5^\circ\text{C}$, $\theta_A \approx 16^\circ\text{C}$) on this diagram, indicating that the layer is well mixed. Newly entrained parcels would be easily identified as they have lower r_v and θ_W values but higher θ_A values. Figure 4 shows the liquid water mixing ratio profile during RF02/PF04 (a descending sounding through the cloud layer), taken about 40 minutes after the previous sounding (PF03). Both the cloud base and top heights are similar to the previous sounding. Entrainment is still active during this time period. However, the θ_A and θ_W profiles (Figure 5) show a cooling in the cloud layer and in the region immediately below cloud base. The θ_W vs. θ_A diagram of this profile shows that the data points in the cooled layer are aligned in a line parallel to a constant total mixing ratio line. This is an indication that the cooling is caused by long-wave radiative cooling from cloud top. In this figure, data points near cloud top have a saturation pressure level near 1000 mb, which explains the nearly equal values of θ_A and θ_W shown in Figure 5.

3. SUMMARY AND DISCUSSION

From analyzing the DYCOMS-II airborne data, the above-mentioned radiative cooling signatures -- a layer of air, immediately under the inversion base, with cooler θ_A and θ_W values than the air below while the total mixing ratio remains as a constant throughout the boundary layer -- were found periodically in all the research flights. This may be an indication of an intermittent nature of convection in the marine boundary layer. The effect of radiative cooling gradually diffuses downward by turbulent mixing, leading to a hydrostatically unstable layer. Any triggering mechanism may initiate the convective motion that leads to a well-mixed marine boundary layer.

The data suggests a link between these cooling signatures and the rates of cloud-top radiative cooling. Figures 7 and 8 show the long-wave radiative-heating rate profiles for RF01 PF 03 and PF 04, respectively. As seen in the figure, the minimum heating rate at cloud tops for PF03 is -7K hr^{-1} while for PF04, it is -20K hr^{-1} . The cooling signature

appears mostly when the cloud-top heating rate less than -15 K hr^{-1} . When the heating rate is more than -13 K hr^{-1} , no cooling signatures are found.

The intermittent nature of convection in the marine boundary layer and the radiative cooling effect are important in both cloud dynamics and microphysics. During periods with no convection through the whole boundary layer, the effect of entrainment on cloud droplet spectra broadening (Telford and Chai, 1980, Telford and Wagner, 1981, and Telford et al, 1984) may become effective and lead to faster drizzle formation. The effect of the entity-type entrainment mixing will be lost whenever the surface driven convection (either by water vapor flux or heat flux) mixes through the whole marine boundary layer. However, when the surface driven convection is not active, as indicated by the potentially unstable layer created by cloud-top radiative cooling, the entrained entities have time to circulate inside the cloud layer with continuous mixing with surrounding cloudy air that will lead to the broadening of droplet spectra. All of these mechanisms should be considered in numerical models in order to accurately predict the evolution of marine boundary-layer cloud systems.

4. ACKNOWLEDGEMENT

This work is supported by ONR DEPSCoR Program through Award N00014-01-1-0663.

5. REFERENCES

- Stevens, B. and Co-Authors, 2003: Dynamics and chemistry of marine stratocumulus—DYCOMS-II. *Bull. Amer. Meteor. Soc.*, **84**, 579-593.
- Telford, J. W. and S. K. Chai, 1980: A new aspect of condensation theory. *Pure Appl. Geophys.*, **118**, 720-742.
- Telford, J. W. and P. B. Wagner, 1981: Observations of condensation growth determined by entity type mixing. *Pure Appl. Geophys.*, **119**, 934-965.
- Telford, J. W., T. S. Keck, and S. K. Chai, 1984: Entrainment at cloud tops and the droplet spectra. *J. Atmos. Sci.*, **41**, 3170-3179.
- Telford, J. W. and S. K. Chai, 1993: Vertical mixing in clear air and clouds. *J. Appl. Meteor.*, **32**, 700-715.

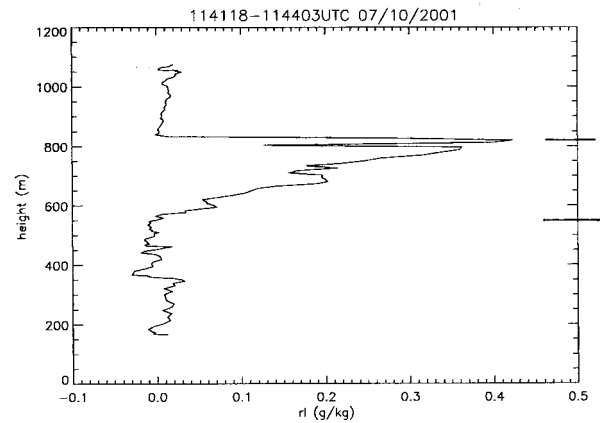


Figure 1 Liquid-water mixing ratio observed during DYCOMS-II Research Flight 01, profile No. 3 (RF01/PF03). Cloud base and top heights are identified by short horizontal lines on the right vertical axis.

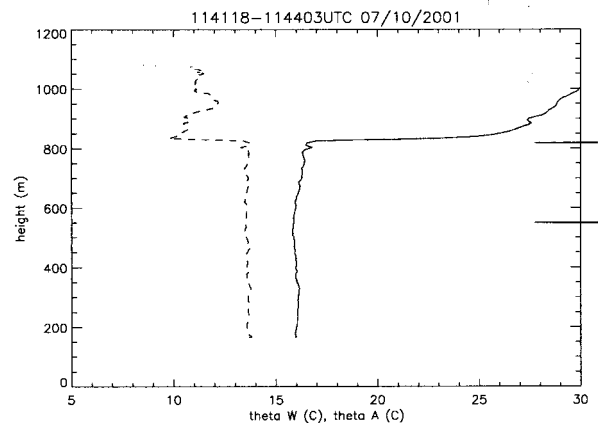


Figure 2 The profiles of absolute potential temperature (solid curve) and wet-bulb potential temperature (dashed curve) of RF01/PF03.

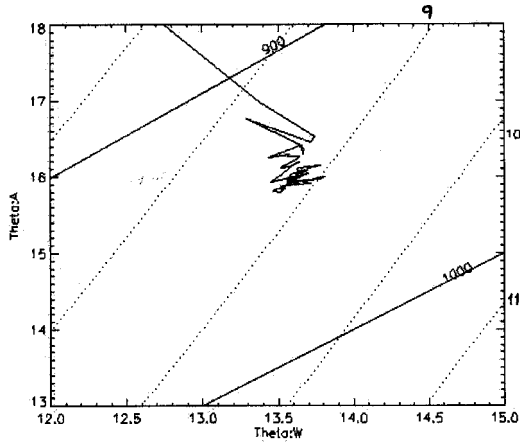


Figure 3 This $\theta_W-\theta_A$ thermodynamic diagram displays the RF01/PF03 data. Since the whole boundary layer is well mixed, the data points measured below the capped temperature inversion are clustered in a small region on this diagram. Solid sloping lines represent constant saturation pressure and the dotted sloping lines represent constant total mixing ratio.

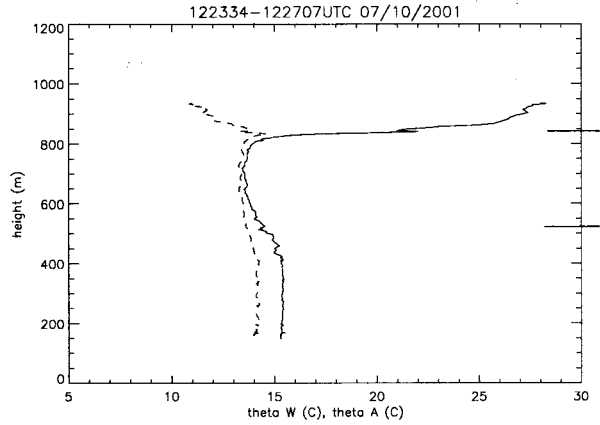


Figure 5 Same as Figure 2 but for RF02/PF04. The cloud layer and the layer immediately below cloud are potentially cooler than the air below. A hydrostatically unstable layer is established from around 400 m up to about 700 m.

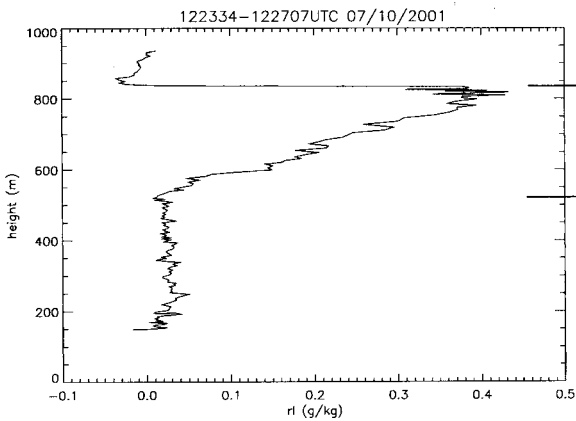


Figure 4 Same as Figure 1 but for RF01/PF04 taken about 40 minutes after the previous sounding.

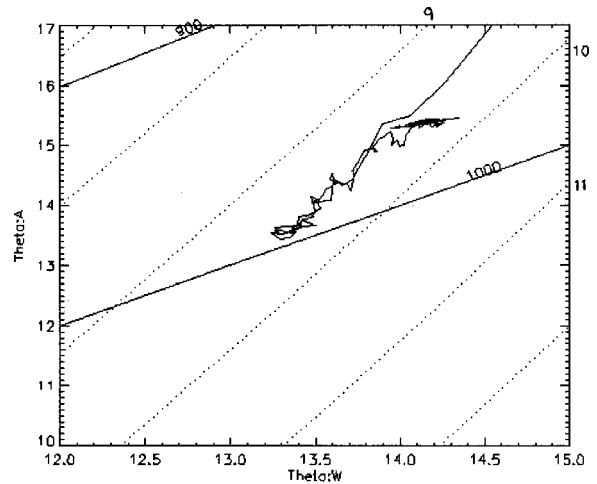


Figure 6 Same as Figure 3 but for RF01/PF04. The data points in the cooled absolute potential temperature region are aligned along a constant total mixing ratio line (dotted lines) indicate that radiative cooling is the main cause of the cooling.

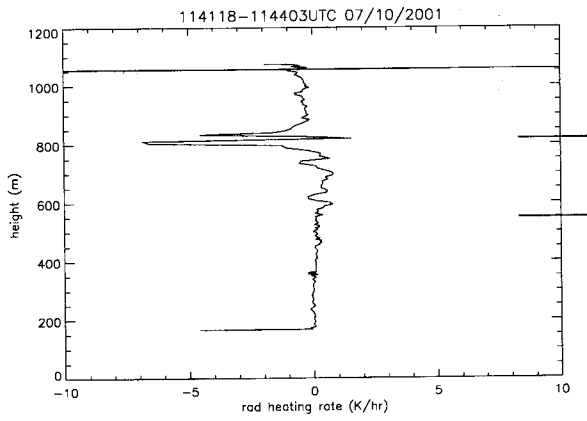


Figure 7 The long-wave radiative heating rate profile for RF01/PF03. The minimum heating rate at cloud top is -7 K hr^{-1} .

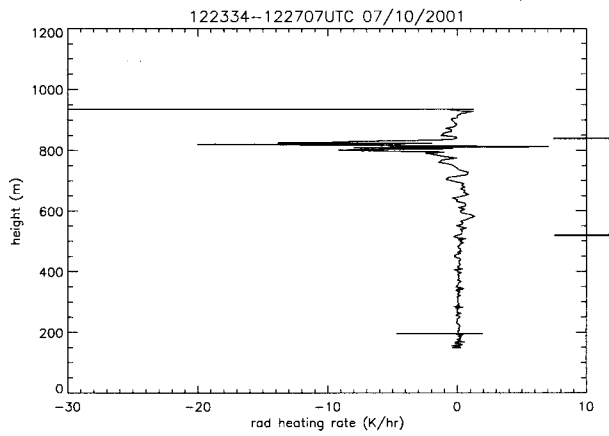


Figure 8 Same as Figure 7 but for RF 01/PF04. The minimum heating rate at cloud top is -20 K hr^{-1} .